Austrian Journal of Earth Sciences | Vienna | 2024 | Volume 117 | 13–24 | DOI: 10.17738/ajes.2024.0002

A thermo-mechanical model of the thermal evolution and incorporation of metamorphic soles in Tethyan ophiolites: a case study from Oman

Iskander Ibragimov[1]*, Daniel Kiss[1,2] and Evangelos Moulas[1]

[1)] Mainz Institute of Multiscale Modelling (M^{3}ODEL) & Institute of Geosciences, Johannes Gutenberg University, Mainz, Germany

[2)] Department of Reservoir Technology, Institute for Energy Technology, Kjeller, Norway

*) corresponding author (iuralovi@uni-mainz.de)

Keywords: ophiolite obduction; metamorphic sole; shear heating; shear zone; Oman ophiolite

Abstract

Ophiolites are remnants of oceanic crust and mantle, now typically found within continental mountain ranges like the Alps. Particularly in areas once part of the Tethys Ocean, ophiolites are often accompanied by narrow stripes of metamorphic rocks, commonly referred to as metamorphic soles. These metamorphic soles typically exhibit peak metamorphic conditions characteristic of either granulite or amphibolite facies. Geochronological studies of Tethyan ophiolites indicate that the development of these metamorphic soles occurred almost simultaneously with the crystallization of the ophiolite's crustal sequence. Geological evidence also suggests that the metamorphism of the sole rocks took place concurrently with deformation, likely at the same time as the ophiolite's obduction. In our research, we explore the metamorphic effects of shearing in an ophiolite sequence overlying a crustal sequence. Our findings reveal that strong lithologies like ophiolites can produce additional heat through the dissipation of mechanical energy, which can potentially explain the high temperatures found in metamorphic-sole rocks. In addition, heating-driven softening of the footwall rocks eventually leads to the migration of the active shear zone from the mantle sequence into the upper crustal domain. This migration may be responsible for the metamorphic sole incorporation at the base of the ophiolite. Finally, we demonstrate that stopping the shearing process rapidly cools these rocks, corresponding with the findings from thermochronological studies from Oman ophiolite.

1. Introduction

Ophiolites are considered to be the remnants of ancient oceanic lithosphere and can now be found on top of continental regions (e.g. Frisch et al., 2011). Numerous studies have concentrated on the presence of ophiolite rocks along the Alpine-Himalayan orogenic belt, as these rocks offer critical support for the existence of oceanic lithosphere that has largely been subducted. Evidence of this is now seen in the remnants of the Tethys Ocean, stretching from the Betics and the Alps in the west (e.g. Graciansky et al., 2011b, 2011a; Le Breton et al., 2021), through the Balkans (e.g. Dimo-Lahitte et al., 2001; Borojević Šoštarić et al., 2014), the Hellenides (e.g. Jones and Robertson, 1991; Rassios and Moores, 2006; Rassios and Dilek, 2009), the Taurides and Pontides (e.g. Karaoğlan et al., 2013; Parlak et al., 2019), and extending to Iran and Oman in the east (Fig. 1; e.g. Garfunkel, 2006; Dilek et al., 2007; Dilek and Furnes, 2019).

Since the early stages of the development of the theory of plate tectonics, the study of ophiolite belts posed significant challenges regarding the mechanisms and the processes that operate during their emplacement or obduction (Dewey, 1976; Moores, 1982). This is because the negative buoyancy of oceanic lithosphere is a dominant force driving plate tectonics (Forsyth and Uyeda, 1975), and it is quite natural that, in active margins, the cold and dense oceanic lithosphere tends to get subducted (Cloos, 1993). However, in many places oceanic lithosphere is obducted. For example, in the European Alps, much of the Mesozoic Penninic ocean lies on top

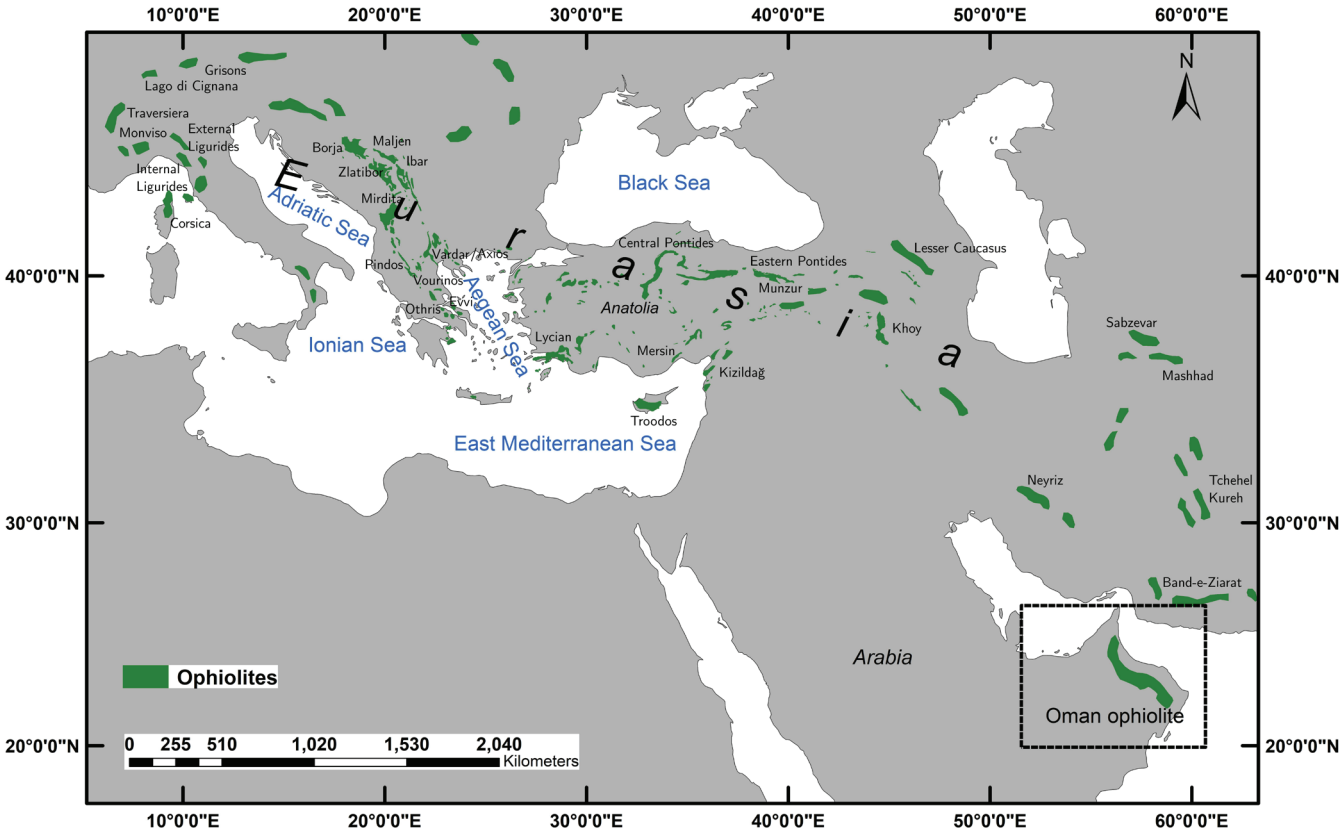

Figure 1: Simplified map showing the distribution of ophiolites in the Mediterranean region. The Oman ophiolite is shown in the lower, right part of the map. Data mostly after Dilek et al. (2007; and references therein).

of the European plate presenting a series of unresolved problems (McCarthy et al. 2018). The subduction of oceanic lithosphere is a process that will erase most of the evidence documenting the former presence of the ocean (Dewey, 1976). Thus, despite their scarcity, ophiolites can help us unravel the processes related to oceanic subduction and mountain building.

The ideal stratigraphic sequences of ophiolites involve (from top to bottom) oceanic sediments, pillow lavas, sheeted dikes, gabbros and ultramafic rocks (Anonymous, 1972, Philpotts and Ague 2022, p. 430). This ideal stratigraphy is mostly not found completely, and different parts of the sections are observed in the Alps or in the Eastern Mediterranean ophiolites (e.g. Bernoulli and Jenkyns, 2009; Rassios and Dilek, 2009). In many cases, crustal metamorphic rocks of mafic or pelitic composition can also be found below the ophiolite complexes (Williams and Smyth, 1973; Whitechurch and Parrot, 1974, 1978; Woodcock and Robertson, 1977; Malpas, 1979; Jamieson, 1980). These rocks are commonly known as metamorphic soles or aureoles (Williams and Smyth, 1973; Malpas, 1979) and are characterized by high-temperature metamorphism in a narrow (tens to hundred meters in thickness) region (Williams and Smyth, 1973; Wakabayashi and Dilek, 2003). The metamorphic conditions that are commonly reported for the soles are amphibolite to granulite facies (e.g. Jamieson, 1980; El-Shazly and Coleman, 1990; Pomonis et al., 2002; Myhill, 2011), and in particular they range between 600–800 °C and 0.5–1.0 GPa.

The pressure and temperature range of the metamorphic conditions have long been a matter of investigation since the metamorphic pressures in the sole rocks typically exceed the burial estimates from geological constraints (Wakabayashi and Dilek, 2000; Garfunkel, 2006). One way to reconcile such discrepancies is to realize that the pressure in the deforming metamorphic sole does not always correspond to the lithostatic value (Moulas et al., 2013). In fact, numerical models for the onset of obduction suggest that the pressure can be up to twice its lithostatic value (Duretz et al., 2016; Fig. 2). Since structures related to exhumation are typically missing (Garfunkel, 2006), non-lithostatic pressure models do not need to explain the missing exhumed structures or the missing eroded material. Nevertheless, the high-grade metamorphic rocks are also thought to have formed inverted metamorphic gradients where the temperature deceases with structural depth (Spray, 1984). In addition, the older isotopic ages from the metamorphic sole rocks are almost indistinguishable from the youngest "magmatic" ages of the ophiolite (Spray and Roddick, 1980; Hacker et al., 1996; Liati et al., 2004; Rioux et al., 2016; Guilmette et al., 2018; Garber et al., 2020). Such observations lead previous authors to conclude that both shear heating and the heat from the young (and hot) mantle

lithosphere contributed to the formation of these rocks (Williams and Smyth, 1973; Woodcock and Robertson, 1977; Malpas, 1979).

Extensive thermochronological analysis performed on metamorphic-sole rocks from Oman has revealed that the cooling of hornblende, amphibole and biotite separates from the sole rocks occurred very fast (Hacker et al., 1996). These cooling rates are variable and range between 100–400 °C per million years for the temperature range of 500–800 °C (Hacker et al., 1996). Such high cooling rates are difficult to be explained using regional exhumation models and suggest the presence of small, local heat sources (Stüwe and Ehlers, 1998; Burg and Moulas, 2022). Thus, the consideration of heat production during the irreversible deformation of rocks may be the reason for the local heat production adjacent to shear zones.

The irreversible deformation of all materials leads to the generation of heat as a consequence of the conservation of energy (Joule and Faraday, 1850; Landau and Lifshitz, 1987; Young, 2015). Indeed, for the Eastern Alps, it has been argued that shear heating provides a contribution to the eoalpine heat budget of the entire Austroalpine nappe pile (Stüwe 1998). This energy can either be diffused away from the main zone of deformation, or can be used to increase the temperature in zones of localized deformation (Gruntfest, 1963; Brun and Cobbold, 1980; Burg and Gerya, 2005; Braeck and Podladchikov, 2007). The local temperature increase leads to the reduction of rheological parameters such as the effective viscosity (e.g. Kaus and Podladchikov, 2006) and critical friction coefficient (e.g. Vardoulakis, 2002). Thus, the local decrease in rheological parameters can result in higher deformation rates and additional weakening of the rock. In general, the heat production per unit volume is proportional to the stress and the strain rate of the deformed material. Thus, many studies have used predefined values for stress and strain rate in shear zones of prescribed (finite or not) thickness (e.g. Reitan, 1968; Graham and England, 1976; Mako and Caddick, 2018). Such models have been very useful since they have been corroborated with natural geologic data (Barton and England, 1979; Petroccia et al., 2022). However, a different category of models can be used that solves for all the thermomechanical parameters needed (c.f. Yuen et al., 1978). In the latter approach one only needs to specify the kinematic boundary conditions (velocity at the boundaries) and it is not required to specify the thickness of the shear zone and its stress. During the simulation, the stress values and the thickness of the shear zone are computed, allowing for the self-regulation of heat generation (Kiss et al., 2019).

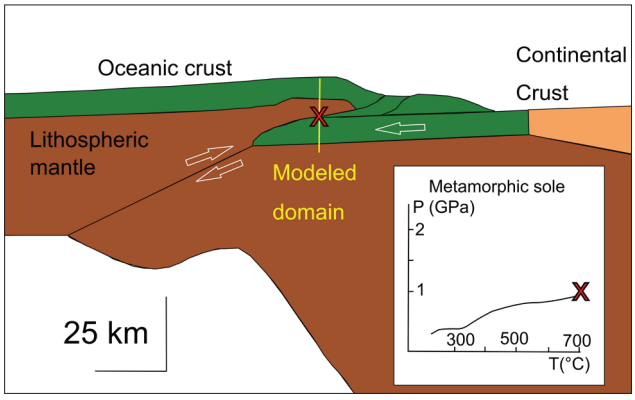

Figure 2: Simplified sketch redrawn to scale after the numerical models of Duretz et al. (2016; their Fig. 3). Our focus region is shown using a thin vertical line. The red cross shows the contact region between the mantle (upper domain) and the crust (lower domain). The inset shows the pressure and temperature conditions of that point (metamorphic sole) at 1.5 Myr after the onset of obduction.

To test the feasibility of shear heating models, we have built upon previous thermomechanical models that simultaneously solve for the stresses and the temperature in a region deforming by simple shear (Yuen et al., 1978; Fleitout and Froidevaux, 1980; Kiss et al., 2019). Our model considers the initial emplacement of a hot mantle rock atop a colder oceanic crustal rock (Fig. 2). More details for the development of the thermomechanical model are given in section 2 (Methods). The initial geothermal gradient used in our model is consistent with the emplacement of a young (and hot) mantle rock on cold crustal lithologies following Hacker et al. (1996). In agreement with previous studies (Hacker, 1990), our results show that the initial shear zone progressively migrates from the upper to the lower plate. This is particularly of interest since it provides a natural mechanism for the incorporation of the metamorphic sole, even if the initial thrust zone was at the lithological boundary. In addition, our results predict that the peak temperature experienced by the sole rocks is a function of the boundary velocity and it is within the range of the observed values for Oman (El-Shazly and Coleman, 1990; Garber et al., 2020) assuming realistic shearing velocities (1–10 cm/yr). Considering this velocity range, a simple scaling relationship can be established based on the systematic results of our study. Last but not least, our model is able to predict a cooling history for the metamorphic-sole rocks that is in excellent agreement with the available thermochronology data from Oman (Hacker et al., 1996).

2. Methods

We begin by considering the deformation along a vertical section following the approach of Yuen et al. (1978) that is described in detail in Burg and Moulas (2022; their Appendix 4). We consider that x_1 is the direction parallel to an initially horizontal shearing plane (and the shearing direction) and x_3 is the direction normal to the shear zone (vertical orientation in our case; Fig. 3). Note that the x_3 direction is pointing upwards whereas depth (z) is pointing downwards (Fig. 3). For this particular orientation of the shear zone and model assumptions, conservation of momentum in the vertical direction reduces to the lithostatic formula (Burg and Moulas, 2022). Therefore, we will not consider pressure effects further since the pressure evolution is a function of the shear-zone orientation (Mou-

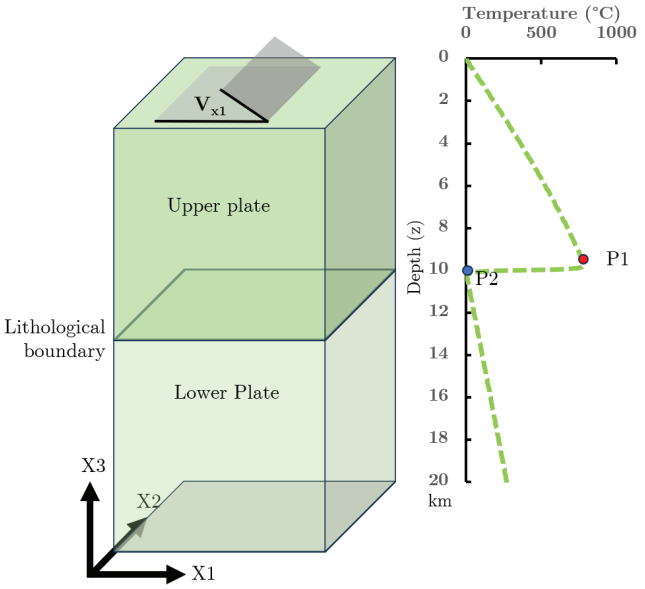

Figure 3: Thermomechanical model configuration. A right-hand coordinate system is also shown (x_1, x_2, x_3). It is assumed that the upper plate has mantle rheology whereas the lower plate has a strong crustal rheology. The initial temperature distribution is shown on the plot on the right as a function of depth (z). Note that the vertical coordinate and the depth are related via $z = L - x_3$, where L is the total length of the model. The points P1 and P2 on the right plot serve to track temperature fluctuations at the base of the upper plate and at the top of the lower plate, respectively.

las et al., 2014, 2022) and its investigation is beyond the scope of this study. Symbols and material constants used in this study are given in Table 1 and Table 2, respectively.

Due to problem's symmetry, all derivatives in the x_1 and x_2 direction vanish. We assume that our material is incompressible and, therefore, the continuity equation reduces to the following form:

$$\frac{\partial v_3}{\partial x_3} = 0 \tag{1}$$

where v_3 is the velocity in the x_3 (vertical) direction. The flow is assumed to be slow (inertial terms are negligible) and viscous, this reduces the momentum conservation along x_1 (parallel to the shearing plane) as follows (Fleitout and Froidevaux, 1980, p. 160):

$$\frac{\partial \tau_{13}}{\partial x_3} = 0 \tag{2}$$

where τ_{13}, is the shear stress within the shear zone. Equation (2) implies that τ_{13} remains constant in the shear zone during deformation. Note however that τ_{13} is constant in space, but not in time. Under these assumptions, the temperature in the shear zone can be given as follows:

$$\rho C_P \frac{\partial T}{\partial t} = \frac{\partial}{\partial x_3}\left(\lambda \frac{\partial T}{\partial x_3}\right) + 2\tau_{13}\dot{\varepsilon}_{13} \tag{3}$$

where, in our case, $\dot{\varepsilon}_{13}$ is given by equation (4):

$$\dot{\varepsilon}_{13} = \frac{1}{2}\left(\frac{\partial v_3}{\partial x_1} + \frac{\partial v_1}{\partial x_3}\right) = \frac{1}{2}\frac{\partial v_1}{\partial x_3} \tag{4}$$

At this point, we can integrate the previous equation with respect to x_3 to obtain:

$$\int_{x_3=0}^{x_3=L'} \dot{\varepsilon}_{13} dx_3 + \int_{x_3=L'}^{x_3=L} \dot{\varepsilon}_{13} dx_3 = \int_{x_3=0}^{x_3=L'} \frac{1}{2}\frac{\partial v_1}{\partial x_3} dx_3 + \int_{x_3=L'}^{x_3=L} \frac{1}{2}\frac{\partial v_1}{\partial x_3} dx_3 = \frac{\Delta V}{2} \tag{5}$$

where L' is the coordinate of the lithological boundary and L is the vertical coordinate of the top surface. The velocity difference between the top surface ($x_3 = L$) and the bottom boundary ($x_3 = 0$) of our model domain is ΔV.

Compared to previous work (Yuen et al., 1978; Fleitout and Froidevaux, 1980; Burg and Moulas, 2022), we considered the following approximation for the non-linear, viscous rheology (creep) of rocks (Tsenn and Carter, 1987, p. 5; Renshaw and Schulson, 2017, p. 15). Note that the following formula is a combination of dislocation and exponential (Peierls) creep:

$$\dot{\varepsilon}_{13} = A_h \sinh(\beta\tau_{13})^n \exp\left(-\frac{Q}{RT}\right) \tag{6}$$

where A_h, β, n and Q are material parameters. The previous formula places a limit on the high stress obtained in the case of fast deformation in a way consistent with exponential creep. The advantage of Equation 6 is that the transition from low-stress creep to exponential creep occurs gradually in agreement with rheology experiments (Renshaw and Schulson, 2017). It can be shown that by choosing $A_h = A/\beta^n$ and $\beta = Q/(RT\sigma_P n)$ one recovers the power-law limit [$\dot{\varepsilon}_{13} = A\tau_{13}^n \exp(-Q/(RT))$] at low stress conditions. Note that σ_P is a material parameter with units of stress for the exponential flow creep (Renshaw and Schulson, 2017). Here, we use 9 GPa (adjusted for stress tensor invariant forms) as for both olivine and anorthite since their σ_P parameters are very similar (Evans and Goetze, 1979; Azuma et al., 2014). Since our model consists of two different regions (Fig. 3), we consider two flow laws of the form shown in Equation 6 consistent with olivine rheology (above) and dry anorthite (below). The rheological parameters are taken from Ranalli, (1995; for olivine) and Rybacki and Dresen, (2004; for anorthite).

To solve the system of equations we assume an initial temperature distribution and we substitute Equation 6 in Equation 5. The result reads (see Tab. 2 for details regarding the symbols used):

$$\int_{x_3=0}^{x_3=L'} A_{h1} \sinh(\beta_1\tau_{13})^{n1} \exp\left(-\frac{Q_1}{RT(x_3)}\right) dx_3 + \cdots$$
$$\int_{x_3=L'}^{x_3=L} A_{h2} \sinh(\beta_2\tau_{13})^{n2} \exp\left(-\frac{Q_2}{RT(x_3)}\right) dx_3 = \frac{\Delta V}{2} \tag{7}$$

The resulting equation can be used to calculate stress (τ_{13}). To perform this calculation, we utilize Newton iterations. The estimated stress (τ_{13}) is then substituted back into Equation 6 to obtain the strain rate distributions for the two domains. Both stress and strain rate distributions are then be substituted into Equation 3 to solve for the temperature update. The temperature distribution is solved via the forward-Euler method using Dirichlet boundary conditions at the top (fixed temperature at 0 ºC) and Neumann boundary conditions (heat flux is prescribed) at the bottom. Due to the non-linear nature of the problem, the timestep of the Euler method is adapted (reduced) automatically in the case of fast temperature rise to avoid numerical instabilities. The bottom heat flux is constrained by our initial temperature distribution that assumes that the temperature in each domain follows a half-space cooling model with different "thermal ages" (ϑ; 2 Myr at the top and 25 Myr at the bottom). The half-space cooling is given by (e.g. Stüwe, 2007):

$$T(°\mathrm{C}) = 1200 \cdot \mathrm{erf}\left(\frac{z}{2\sqrt{\kappa\vartheta}}\right) \quad (8)$$

where is the original depth before the duplication and $\kappa = \lambda/(\rho C_p)$ is the thermal diffusivity. The temperature profile that results after an instantaneous duplication has been criticised as being unphysical (Burg and Moulas, 2022, p. 9). This is because it requires initially infinitely fast velocities (to achieve instantaneous duplication) and, at the same time, it neglects shear heating (that is proportional to shearing velocity). For this reason, we calculate the duplicated temperature distribution by assuming an initial temperature diffusion for a period of 1000 years. This initial diffusion step ignores the contributions from shear heating during the initial stage of the duplication.

To be able to compare our results with the observed cooling rates, we considered that the shearing operates only for a given amount of time, after which the temperature just diffuses. In our case, we consider that the shearing lasted for 1.4 Myr. This choice was made since numerical models have shown that the initial duplication and the formation of metamorphic sole occurred within 1.5 Myr (Duretz et al., 2016; their Fig. 3). Overall, the temperatures calculated by the model are calculated until 4.4 Myr.

Parameter	Symbol	Units
Temperature	T	$°C$ *or* K
Deviatoric stress tensor	τ_{ij}	Pa
Velocity	v_i	$\mathrm{m\ s^{-1}}$
Density	ρ	$\mathrm{kg\ m^{-3}}$
Spatial coordinate (measured from bottom)	x_i	m
Depth (measured from top)	z	m
Total length of model	L	m
Peierls stress	σ_P	Pa
Specific heat	C_p	$\mathrm{J\ kg^{-1}\ K^{-1}}$
Thermal conductivity	λ	$\mathrm{J\ m^{-1}\ s^{-1}\ K^{-1}}$
Thermal diffusivity	κ	$\mathrm{m^2\ s^{-1}}$
Material constant (used in viscous flow law)	A_0	$\mathrm{Pa^{-n}\ s^{-1}}$
Stress exponent (used in viscous flow law)	n	–
Activation energy (used in viscous flow law)	Q	$\mathrm{J\ mol^{-1}}$
Gas constant	R	$\mathrm{J\ mol^{-1}K^{-1}}$

Table 1: Symbols and units of quantities used in this study.

Parameter	Symbol	Value
Total length of model	L	20000
Peierls stress	σ_P	$9.9 \cdot 10^9 \cdot 3^{-\frac{1}{2}}$
Specific heat (upper domain)	C_{p2}	1050
Specific heat (lower domain)	C_{p1}	1050
Thermal conductivity (upper domain)	λ_2	3.0
Thermal conductivity (lower domain)	λ_1	2.2
Thermal diffusivity (upper domain)	κ_2	$8.4 \cdot 10^{-7}$
Thermal diffusivity (lower domain)	κ_1	$7.9 \cdot 10^{-7}$
Material constant (used in viscous flow law) (upper domain)	A_{02}	$2.5 \cdot 10^{-21}$
Material constant (used in viscous flow law) (lower domain)	A_{01}	$5.01 \cdot 10^{-6}$
Stress exponent (used in viscous flow law) (upper domain)	n_2	3.5
Stress exponent (used in viscous flow law) (lower domain)	n_1	3.0
Activation energy (used in viscous flow law) (upper domain)	Q_2	$5.32 \cdot 10^5$
Activation energy (used in viscous flow law) (lower domain)	Q_1	$6.56 \cdot 10^5$
Gas constant	R	8.314

Table 2: Values of parameters that have been used in this study.

3. Results

We have performed 5100 simulations to determine the effects of boundary velocities and boundary conditions. However, we have chosen a specific model as our reference to provide a detailed description. The reference model results are given in Figures 4–6.

3.1 Temperature of the shear zone

Our results show that, with the initiation of shearing, there is a region at about 8 km depth where temperature initially grows with time (Fig. 4a). This temperature growth is attributed to the increased dissipative heating within the upper plate. The zone of increased dissipative heating is the zone of fastest deformation (Fig. 4d), which generally does not stay fixed in space. As time progresses, the main zone of heat production moves towards the lower plate. This can be deduced by the fact that the temperature and the strain rate peaks are now below the lithological boundary (Fig. 4b,e). Since the shearing lasts for only 1.4 Myr, there is no heat production beyond this point. Thus, the temperature distribution relaxes following a purely conductive behaviour (Fig. 4c). This is also shown by the fact that the strain rate after 1.4 Myr is zero (Fig. 4f). The maximum temperature (T_{max}) experienced by the rocks in the whole modelled history is shown with a blue, solid line in Figure 4c. The results show that the

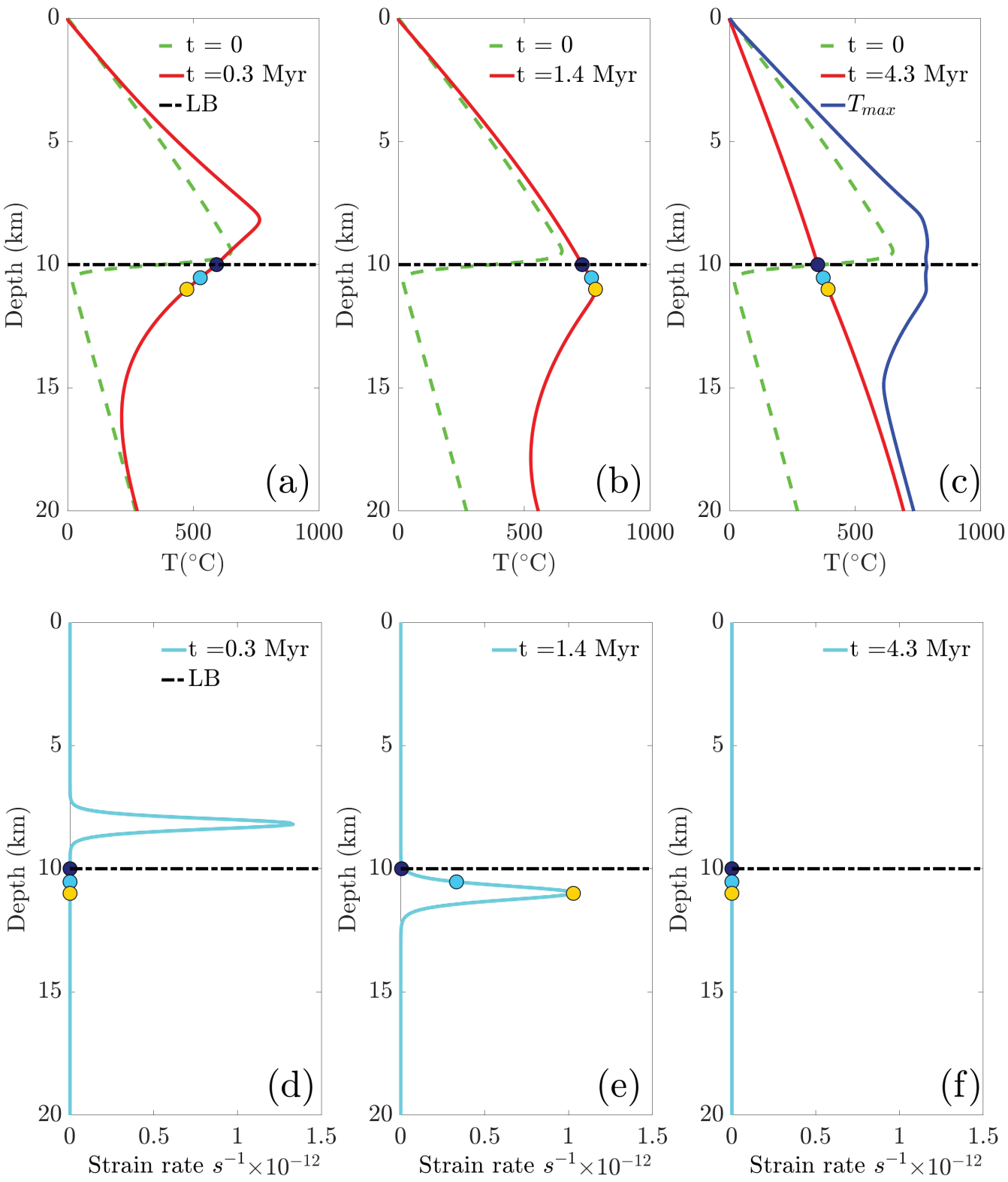

Figure 4: Temperature (T) evolution (a,b,c) and strain rate ($\dot{\varepsilon}_{13}$) distribution (d,e,f) with time. The horizontal, black dashed line indicates the position of the lithological boundary. **(a)** Temperature distribution 0.3 Myr after the shearing initiation, **(b)** at the end of shearing (1.4 Myr), **(c)** at a time of 4.3 Myr. The initial temperature distribution is given with a green dashed line. The maximum temperature (T_{max}) recorded by every point of the whole profile is shown using a blue solid line. **(d)** Strain rate distribution at the onset of shearing (0.3 Myr), (e) at 1.4 Myr, **(f)** at 4.3 Myr.

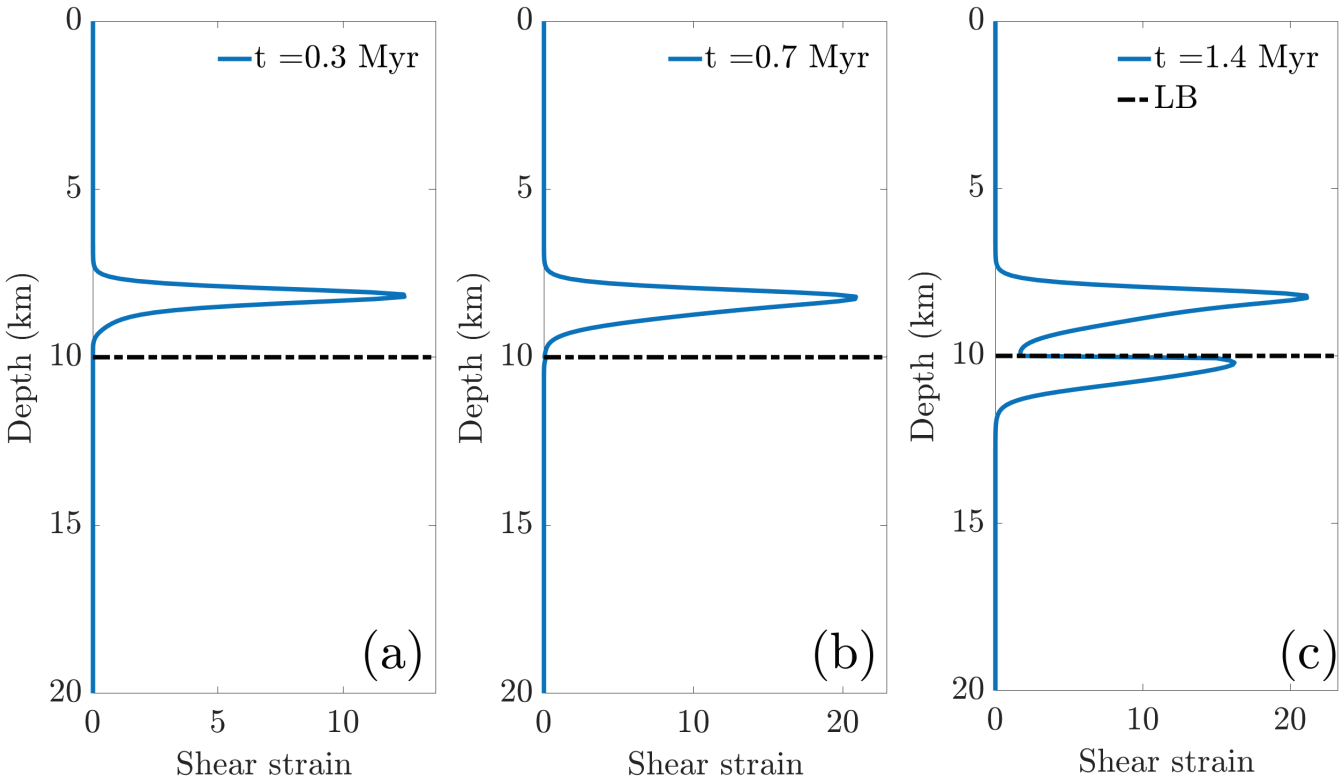

Figure 5: Finite shear strain evolution as a function of time after the shearing initiation. Shear strain has been calculated as the time integral of the shear strain rate ($\int \dot{\varepsilon}_{13} dt$). The horizontal, black dashed line indicates the position of the lithological boundary. **(a)** Finite shear strain at 0.3 Myr, **(b)** at 0.7 Myr, **(c)** at 1.4 Myr (end of shearing).

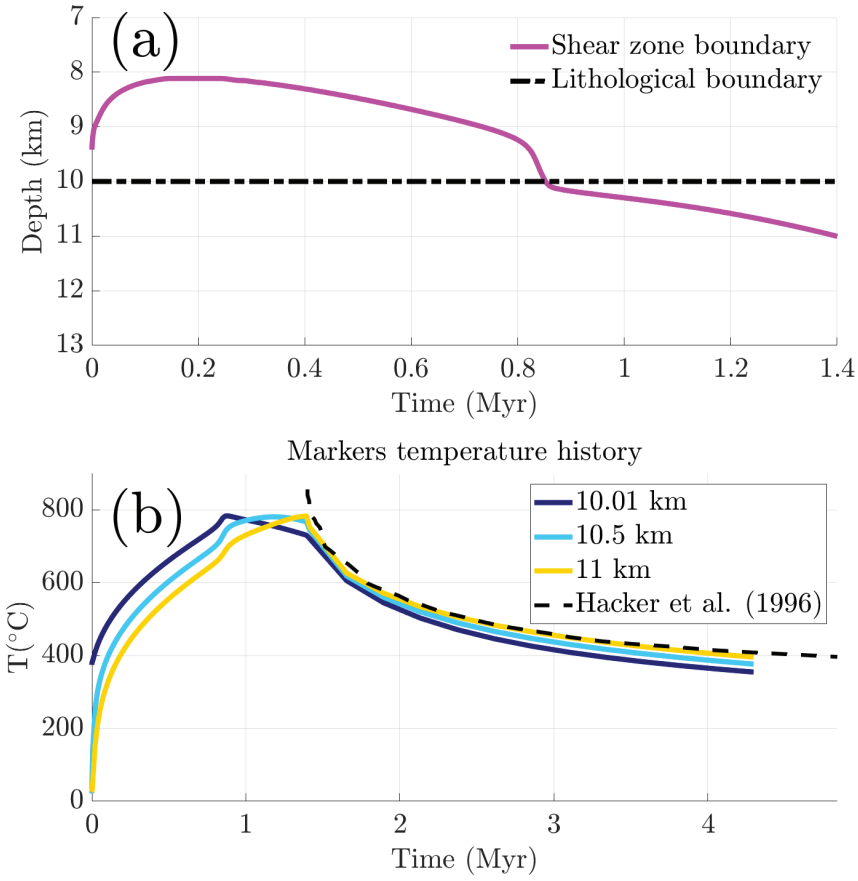

Figure 6: (a) Depth of the active shear zone with time. The depth of the shear zone is taken as the maximum of the strain rate ($\dot{\varepsilon}_{13}$) distribution at each time. The horizontal, dashed line indicates the position of the lithological boundary. **(b)** Temperature history of markers in the vicinity of the lithological boundary. The cooling history that has been inferred by Hacker et al. (1996) is shown using a dashed black line.

rocks in the vicinity of the lithological boundary experienced temperatures in the order of 800 °C. More specifically, the maximum temperature in the reference model was about 783 °C. We note that the (T_{max}) distribution does not correspond to the temperature of a particular time instance.

3.2 Shear zone migration

The migration of the temperature maximum with time shown in Figure 4 is attributed to the migration of the main shear zone as time progresses (Fig. 5). The reason for this migration is the heat conduction from the, initially hotter, upper plate towards the lower plate. To be more specific, as the upper plate cools and the lower plate heats up simultaneously, this process gradually decreases the lower plate's effective viscosity. This viscosity reduction is responsible for the localization of the shear zone at different depths. The distribution of the finite shear strain after 0.3, 0.7 and 1.4 Myr shows that the shear zone developed first in the upper plate and finally migrated in the lower plate (Fig. 5). In fact, the migration of the active shear zone occurs in a progressive manner as it is shown in Figure 6a. Such migration of the shear zone would be responsible for the accretion of the upper part of the oceanic upper plate at the base of the former upper plate.

3.3 Cooling-rate constraints

One extraordinary feature from the metamorphic-sole rocks of Oman is the very high cooling rates inferred for the metamorphic minerals (Hacker et al., 1996, p. 1242). This shape of cooling path and the high cooling rates are characteristic for the rapid cooling of shear-zone rocks (Burg and Moulas, 2022, p. 11). For this reason, we have considered that the shearing occurs only for a finite period of time. As it was mentioned earlier, the shearing in the reference model occurred only for a period of 1.4 Myr. This value is consistent with values of ophiolite obduction and metamorphic sole formation (Duretz et al., 2016). However, we would like to note that it is not necessary for the velocity to be zero after this initial period of 1.4 Myr. Smaller values of velocity could still operate and the material could shear but without a significant heat production. Thus, this value should be viewed as a period of intense shearing and not as the total period of shearing. The temperature evolution of rocks found in the vicinity of the initial lithological boundary is shown in Figure 6b. Our thermal-history results (solid lines; Fig. 6b) show an exceptionally good fit when compared to the thermal histories (dashed black line; Fig. 6b) inferred using thermochronology data (Hacker et al., 1996, p. 1242). These results also show that the highest cooling rates are expected immediately after the cessation of shearing.

3.4 Systematic investigations

Since the maximum temperature in our results is always found in the region close to the lithological boundary (e.g. Fig. 4c), we have performed systematic investigations to get more insights on the thermal evolution of the rocks in that region. In these investigations, the shearing duration is assumed to be fixed at 1.4 Myr and we report the average temperature within 10 m from the lithological boundary (above and below). Our results show that there is a strong dependence of the maximum temperature on the initial age of the ocean, especially for oceanic lithosphere that is younger than 2 Myr (Fig. 7a). This is probably because the oceanic crust is still too hot to localize deformation and most of the heating of the lower plate occurs via conduction from the upper domain. Beyond the age of 2 Myr, our results show that the age of the ocean in the upper plate is not an important parameter regarding the maximum temperature of the shear-zone rocks (Fig. 7a). In contrast, the shearing velocity plays the most dominant role in the rising of the maximum temperature (Fig.7a). It is noted that only 2.5 cm/yr shearing velocity is sufficient to bring the temperature above 700 °C (Fig. 7a). For the reference model, the maximum temperature is around 783 °C (red star; Fig. 7a). Increasing the shearing velocity beyond this level does not bring a dramatic increase on the maximum temperature value.

The relatively simple dependence of the maximum temperature on the shearing velocity allows us to deduce a simple relation from our results. By using bilinear-least squares fitting, the maximum temperature (T) data shown in Figure 7a can be described by the following relation:

$$T[°\mathrm{C}] = -2.0104 \cdot A_o[\mathrm{Myr}] + 189.9315 \cdot log_{10}(\Delta V[\mathrm{cm} \cdot \mathrm{yr}^{-1}]) + 924.6811 \quad (9)$$

where (A_o) is the age of the ocean in Myr and ΔV is the velocity of shearing in cm/yr. This simple formula applies for velocities larger than or equal to 1.5 cm/yr and for ocean ages older than 2 Myr. Equation 9 can reproduce the data of Figure 7a within 19 °C (maximum error). The mean absolute error of Equation 9 is only 3.6 °C.

Finally, to see the effect of shear heating on the thermal model, we have also plotted the difference between the maximum temperature obtained using a thermo-mechanical model and the maximum temperature of a pure thermal (i.e. conductive) model (Fig. 7b). All other parameters (initial conditions, thermal parameters) remain the same as in the reference model. The results show that for our reference conditions, a purely thermal model predicts about 335 °C lower peak metamorphic temperatures, which is much lower than what is observed in the metamorphic sole of the Oman ophiolite.

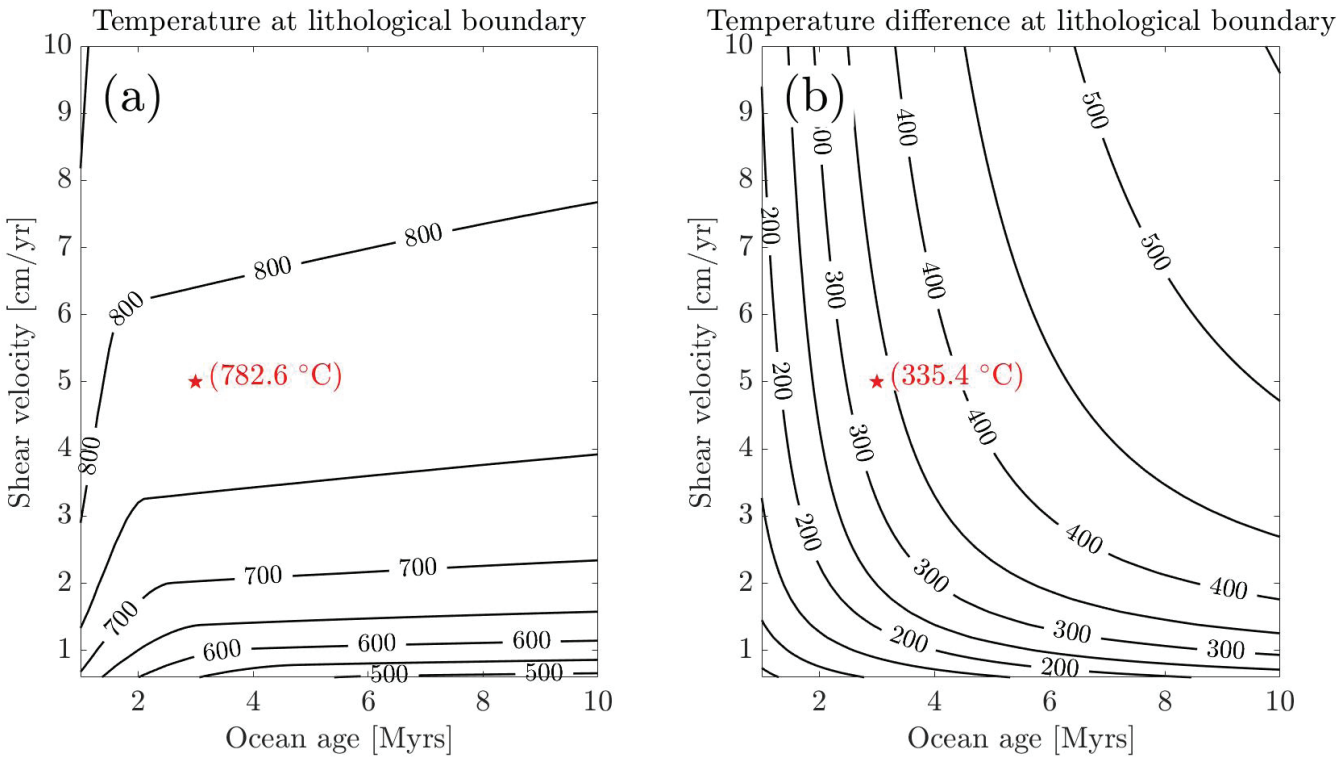

Figure 7: (a) Maximum temperature at the vicinity of the lithological boundary (±10 m) as a function of the age of the ocean (in Myr) and of the shearing velocity (in cm/yr). The red star indicates the parameters of the reference model (Figs. 4–6). The value in parentheses indicate the maximum temperature value of the reference run. **(b)** Temperature difference from a purely thermal model as a function of the same parameters as in (a). The reference run is indicated by a red star and the value in the brackets indicates the temperature difference from the purely thermal model.

4. Discussion

For many years, researchers have considered shear (viscous or frictional) heating as a mechanism for generating the necessary temperature conditions required for the metamorphism of ophiolite soles (Woodcock and Robertson, 1977). One of the challenges for this interpretation, however, is that most of the ophiolite soles are almost contemporaneous with the crustal sequence of the ophiolites above them. This relationship has been interpreted to reflect the fact that the oceanic lithosphere must be young (and hot) to be able to be obducted on the continent (Spray, 1984; Wakabayashi and Dilek, 2003; Parlak et al., 2019). Recent thermomechanical models support that it is possible to obduct a hot and young oceanic lithosphere on the continental margin (Duretz et al., 2016; Ibragimov and Moulas, 2024). Therefore, the heat conducted from the young oceanic plate can be sufficient to explain the high-temperature metamorphic aureole beneath the ophiolite (England and Molnar, 1993). One of the problems of the previous interpretation is related to the fact that the obducted oceanic lithosphere must be hot at the time that it is positioned on top of the crustal sequence. This requires that the tectonic movements are fast, and since shear heating scales proportional to the shearing velocity, shear heating cannot be excluded in modelling this process (Duprat-Oualid et al., 2015). Thus, models that include shear heating are needed to quantify the heating from the overriding plate towards the footwall during obduction. Then, for each case, the importance of shear heating would be a model result and not an a-priori assumption.

One of the main assumptions in our work is the incorporation of a strong, crustal rheology (Rybacki and Dresen, 2004). We have modified the high-stress limit of this rheology by employing a hyperbolic-sine flow law that approximates exponential creep at high stresses (Tsenn and Carter, 1987; Renshaw and Schulson, 2017). This modification is needed to maintain reasonable levels of stress that would not grow beyond the strength of the material for the given shear velocities. It is possible however that the material of the hanging wall had a relatively softer rheology that would not allow the localization of deformation due to thermal softening. In such a case, the peak temperatures obtained would be significantly lower (Kiss et al., 2019).

When using a strong crustal rheology, as in our case, our models (Fig. 7a) revealed that velocities larger than 2 cm/yr are sufficient to generate metamorphic conditions that are in agreement with the values and the apparent metamorphic gradients reported in Oman and in other ophiolites in general (e.g. El-Shazly and Coleman, 1990; Jamieson, 1980). In fact, if shear heating was not considered, then the maximum temperature in the same region would be approximately 335 °C lower (Fig. 7b),

and therefore it would not fit geological data. The fact that both the peak temperatures and the cooling rates are in agreement with the published data (Fig. 6b) suggests that our choice of conditions and parameters is realistic for the case of Oman ophiolite.

One limitation of our model is that it did not consider the effects of shear heating during the initial duplication stage (first 1000 years). This is because it is not possible to create a duplication out of a vertical section in a 1-dimensional model. Our model is thus conservative when it comes to the net amount of shear heating. However, our value of 1.4 Myr of intense shearing is very close to the time instance of 1.5 Myr presented in Duretz et al. (2016; their Fig. 3, top panel). In their model, the formation of the high-temperature metamorphic sole takes place before 1.5 Myr (Duretz et al., 2016, p. 5).

The fact that shear heating is important in our models, does not exclude the fact that heat is conducted from the hot, overriding plate towards the relatively cold footwall. This is, in fact, the reason for the migration of the active shear zone at depths lower within the footwall (Fig. 6a). As a result of the shear zone migration, the hanging wall incorporates parts that were originally at the uppermost levels of the initial footwall (crustal domain). Therefore, we suggest that the combination of shear heating and heat conduction of a hot upper plate responsible for: i) the high-temperature metamorphic conditions, ii) the apparent metamorphic inversion observed along the section, iii) the large cooling rates inferred in those rocks, and iv) the occurrence of the metamorphic sole below the mantle sequence.

5. Conclusions

In this study, we introduced new thermomechanical models that are pertinent to the study of ophiolite obduction. These models calculate stress, strain rate, and temperature distributions within a rock segment subjected to simple shear, consisting of two distinct lithologies. Our findings indicate that integrating shear heating in a self-consistent manner yields maximum temperature and cooling-rate predictions that align with natural data. Focusing on Oman as an example, our analysis supports the notion that the high cooling rates deduced from thermochronological data are compatible with the fast cooling following the end of deformation. Additionally, our results demonstrate that thermal softening in the footwall during obduction triggers the shift of the primary shear zone into the footwall material. This shift ultimately leads to the incorporation of the metamorphic-sole rocks at the base of the ophiolite. We suggest that our results may have implications to the Paleogene metamorphism of the rocks underneath the Penninic units in the Tauern window.

Acknowledgements

We would like to thank the Deutsche Forschungsgemeinschaft (DFG) - Project number 512790090 for support related to the development of the methods in this project. K. Stüwe is acknowledged for encouraging us to submit our results to AJES. D.K. acknowledges the European Research Council (Consolidator Grant 771143 (MAGMA) awarded to B.J.P. Kaus), and the Research Council of Norway and the industry partners of NCS2030 (RCN project number 331644) for their support. The authors would like to thank the constructive comments from the editor, M. Adamuszek, R. Carosi, and from an anonymous reviewer, all of which allowed us to improve our manuscript.

References

Anonymous, 1972. Penrose Field Conference on ophiolites. Geotimes 17, 24–25.

Azuma, S., Katayama, I., Nakakuki, T., 2014. Rheological decoupling at the Moho and implication to Venusian tectonics. Scientific Reports 4, 4403. https://doi.org/10.1038/srep04403

Barton, C.M., England, P.C., 1979. Shear heating at the Olympos (Greece) thrust and the deformation properties of carbonates at geological strain rates. Geological Society of America Bulletin 90, 483. https://doi.org/10.1130/0016-7606(1979)90<483:SHATOG>2.0.CO;2

Bernoulli, D., Jenkyns, H.C., 2009. Ophiolites in ocean-continent transitions: From the Steinmann Trinity to sea-floor spreading. Transition Océan-Continent 341, 363–381. https://doi.org/10.1016/j.crte.2008.09.009

Borojević Šoštarić, S., Palinkaš, A.L., Neubauer, F., Cvetković, V., Bernroider, M., Genser, J., 2014. The origin and age of the metamorphic sole from the Rogozna Mts., Western Vardar Belt: New evidence for the one-ocean model for the Balkan ophiolites. Lithos 192–195, 39–55. https://doi.org/10.1016/j.lithos.2014.01.011

Braeck, S., Podladchikov, Y.Y., 2007. Spontaneous Thermal Runaway as an Ultimate Failure Mechanism of Materials. Physical Review Letters 98, 095504-1-4.

Brun, J.P., Cobbold, P.R., 1980. Strain heating and thermal softening in continental shear zones: a review. Journal of Structural Geology 2, 149–158. https://doi.org/10.1016/0191-8141(80)90045-0

Burg, J.-P., Gerya, T.V., 2005. The role of viscous heating in Barrovian metamorphism of collisional orogens: thermomechanical models and application to the Lepontine Dome in the Central Alps. Journal of Metamorphic Geology 23, 75–95. https://doi.org/10.1111/j.1525-1314.2005.00563.x

Burg, J.-P., Moulas, E., 2022. Cooling-rate constraints from metapelites across two inverted metamorphic sequences of the Alpine-Himalayan belt; evidence for viscous heating. Journal of Structural Geology 156, 104536. https://doi.org/10.1016/j.jsg.2022.104536

Cloos, M., 1993. Lithospheric buoyancy and collisional orogenesis: Subduction of oceanic plateaus, continental margins, island arcs, spreading ridges, and seamounts. GSA Bulletin 105, 715–737. https://doi.org/10.1130/0016-7606(1993)105<0715:LBACOS>2.3.CO;2

Dewey, J.F., 1976. Ophiolite obduction. Tectonophysics 31, 93–120. https://doi.org/10.1016/0040-1951(76)90169-4

Dilek, Y., Furnes, H., 2019. Tethyan ophiolites and Tethyan seaways. Journal of the Geological Society 176, 899–912. https://doi.org/10.1144/jgs2019-129

Dilek, Y., Furnes, H., Shallo, M., 2007. Suprasubduction zone ophiolite formation along the periphery of Mesozoic Gondwana. Gondwana Research 11, 453–475. https://doi.org/10.1016/j.gr.2007.01.005

Dimo-Lahitte, A., Monié, P., Vergély, P., 2001. Metamorphic soles from the Albanian ophiolites: Petrology, 40Ar/39Ar geochronology, and geodynamic evolution. Tectonics 20, 78–96. https://doi.org/10.1029/2000TC900024

Duprat-Oualid, S., Yamato, P., Schmalholz, S.M., 2015. A dimensional analysis to quantify the thermal budget around lithospheric-scale shear zones. Terra Nova 27, 163–168. https://doi.org/10.1111/ter.12144

Duretz, T., Agard, P., Yamato, P., Ducassou, C., Burov, E.B., Gerya, T.V., 2016. Thermo-mechanical modeling of the obduction process based on the Oman Ophiolite case. Gondwana Research 32, 1–10. https://doi.org/10.1016/j.gr.2015.02.002

El-Shazly, A.K., Coleman, R.G., 1990. Metamorphism in the Oman Mountains in relation to the Semail ophiolite emplacement. Geological Society, London, Special Publications 49, 473–493. https://doi.org/10.1144/GSL.SP.1992.049.01.30

England, P., Molnar, P., 1993. The interpretation of inverted metamorphic isograds using simple physical calculations. Tectonics 12, 145–157. https://doi.org/10.1029/92TC00850

Evans, B., Goetze, C., 1979. The temperature variation of hardness of olivine and its implication for polycrystalline yield stress. Journal of Geophysical Research: Solid Earth 84, 5505–5524. https://doi.org/10.1029/JB084iB10p05505

Fleitout, L., Froidevaux, C., 1980. Thermal and mechanical evolution of shear zones. Journal of Structural Geology 2, 159–164. https://doi.org/10.1016/0191-8141(80)90046-2

Forsyth, D., Uyeda, S., 1975. On the Relative Importance of the Driving Forces of Plate Motion*. Geophysical Journal of the Royal Astronomical Society 43, 163–200. https://doi.org/10.1111/j.1365-246X.1975.tb00631.x

Frisch, W., Meschede, M., Blakey, R., 2011. Plate Tectonics: Continental Drift and Mountain Building. Springer. https://doi.org/10.1007/s00445-011-0538-0

Garber, J.M., Rioux, M., Kylander-Clark, A.R.C., Hacker, B.R., Vervoort, J.D., Searle, M.P., 2020. Petrochronology of Wadi Tayin Metamorphic Sole Metasediment, With Implications for the Thermal and Tectonic Evolution of the Samail Ophiolite (Oman/UAE). Tectonics 39, e2020TC006135. https://doi.org/10.1029/2020TC006135

Garfunkel, Z., 2006. Neotethyan ophiolites: formation and obduction within the life cycle of the host basins. Geological Society, London, Special Publications 260, 301–326. https://doi.org/10.1144/GSL.SP.2006.260.01.13

Graciansky, P.-C.D., Roberts, D.G., Tricart, P., 2011a. Chapter Eleven - Liguro-piemontais Ophiolites and the Alpine Palaeo-Ocean. In: Pierre-Charles De Graciansky, D.G.R. and P.T. (Ed.), Developments in Earth Surface Processes. Elsevier, 205–242. https://doi.org/10.1016/S0928-2025(11)14011-0

Graciansky, P.-C.D., Roberts, D.G., Tricart, P., 2011b. Chapter Fourteen - The Birth of the Western and Central Alps: Subduction, Obduction, Collision. In: Pierre-Charles De Graciansky, D.G.R. and P.T. (Ed.), Developments in Earth Surface Processes. Elsevier, 289–315. https://doi.org/10.1016/S0928-2025(11)14014-6

Graham, C.M., England, P.C., 1976. Thermal regimes and regional metamorphism in the vicinity of overthrust faults: an example of shear heating and inverted metamorphic zonation from southern California. Earth and Planetary Science Letters 31, 142–152. https://doi.org/10.1016/0012-821X(76)90105-9

Gruntfest, I.J., 1963. Thermal Feedback in Liquid Flow; Plane Shear at Constant Stress. Transactions of the Society of Rheology 7, 195–207. https://doi.org/10.1122/1.548954

Guilmette, C., Smit, M.A., van Hinsbergen, D.J.J., Gürer, D., Corfu, F., Charette, B., Maffione, M., Rabeau, O., Savard, D., 2018. Forced subduction initiation recorded in the sole and crust of the Semail Ophiolite of Oman. Nature Geoscience 11, 688–695. https://doi.org/10.1038/s41561-018-0209-2

Hacker, B.R., 1990. Simulation of the metamorphic and deformational history of the metamorphic sole of the Oman Ophiolite. Journal of Geophysical Research: Solid Earth 95, 4895–4907. https://doi.org/10.1029/JB095iB04p04895

Hacker, B.R., Mosenfelder, J.L., Gnos, E., 1996. Rapid emplacement of the Oman ophiolite: Thermal and geochronologic constraints. Tectonics 15, 1230–1247. https://doi.org/10.1029/96TC01973

Ibragimov, I., Moulas, E., 2024. Role of continental margin architecture in models of ophiolite emplacement. Journal of the Geological Society 181, jgs2023-063. https://doi.org/10.1144/jgs2023-063

Jamieson, R.A., 1980. Formation of metamorphic aureoles beneath ophiolites - Evidence from the St. Anthony Complex, Newfoundland. Geology 8, 150–154. https://doi.org/10.1130/0091-7613(1980)8<150:FORABO>2.0.CO;2

Jones, G., Robertson, A., 1991. Tectono-stratigraphy and evolution of the Mesozoic Pindos ophiolite and related units, northwestern Greece. Journal of the Geological Society 148, 267. https://doi.org/10.1144/gsjgs.148.2.0267

Joule, J.P., Faraday, M., 1850. III. On the mechanical equivalent of heat. Philosophical Transactions of the Royal Society of London 140, 61–82. https://doi.org/10.1098/rstl.1850.0004

Karaoğlan, F., Parlak, O., Klötzli, U., Koller, F., Rızaoğlu, T., 2013. Age and duration of intra-oceanic arc volcanism built on a suprasubduction zone type oceanic crust in southern Neotethys, SE Anatolia. Slab Window Magmatism and Convergent Margin Tectonics 4, 399–408. https://doi.org/10.1016/j.gsf.2012.11.011

Kaus, B.J.P., Podladchikov, Y.Y., 2006. Initiation of localized shear zones in viscoelastoplastic rocks. Journal of Geophysical Research: Solid Earth 111, B04412. https://doi.org/10.1029/2005JB003652

Kiss, D., Podladchikov, Y., Duretz, T., Schmalholz, S.M., 2019. Spontaneous generation of ductile shear zones by thermal softening: Localization criterion, 1D to 3D modelling and application to the lithosphere. Earth and Planetary Science Letters 519, 284–296. https://doi.org/10.1016/j.epsl.2019.05.026

Landau, L.D., Lifshitz, E.M., 1987. Course of theoretical Physics - Fluid Mechanics, 2nd ed. Pergamon. https://doi.org/10.1016/B978-0-08-033933-7.50007-6.

Le Breton, E., Brune, S., Ustaszewski, K., Zahirovic, S., Seton, M., Müller, R.D., 2021. Kinematics and extent of the Piemont-Liguria Basin – implications for subduction processes in the Alps. Solid Earth 12, 885–913. https://doi.org/10.5194/se-12-885-2021

Liati, A., Gebauer, D., Fanning, C.M., 2004. The age of ophiolitic rocks of the Hellenides (Vourinos, Pindos, Crete): first U-Pb ion microprobe (SHRIMP) zircon ages. Chemical Geology 207, 171–188. https://doi.org/10.1016/j.chemgeo.2004.02.010

McCarthy, A., Chelle-Michou, C., Müntener, O., Arculus, R. and Blundy, J. 2018. Subduction initiation without magmatism: The case of the missing Alpine magmatic arc. Geology, 46, 1059–1062, https://doi.org/10.1130/G45366.1.

Mako, C.A., Caddick, M.J., 2018. Quantifying magnitudes of shear heating in metamorphic systems. Tectonophysics 744, 499–517. https://doi.org/10.1016/j.tecto.2018.07.003

Malpas, J., 1979. The dynamothermal aureole of the Bay of Islands ophiolite suite. Canadian Journal of Earth Sciences 16, 2086–2101. https://doi.org/10.1139/e79-198

Moores, E.M., 1982. Origin and emplacement of ophiolites. Reviews of Geophysics 20, 735–760. https://doi.org/10.1029/RG020i004p00735

Moulas, E., Burg, J.-P., Podladchikov, Y., 2014. Stress field associated with elliptical inclusions in a deforming matrix: Mathematical model and implications for tectonic overpressure in the lithosphere. Tectonophysics 631, 37–49. https://doi.org/10.1016/j.tecto.2014.05.004

Moulas, E., Kaus, B., Jamtveit, B., 2022. Dynamic pressure variations in the lower crust caused by localized fluid-induced weakening. Communications Earth & Environment 3, 157. https://doi.org/10.1038/s43247-022-00478-7

Moulas, E., Podladchikov, Y.Y., Aranovich, L.Y., Kostopoulos, D.K., 2013. The problem of depth in geology: When pressure does not translate into depth. Petrology 21, 527–538. https://doi.org/10.1134/S0869591113060052

Myhill, R., 2011. Constraints on the evolution of the Mesohellenic Ophiolite from subophiolitic metamorphic rocks. Geological Society of America Special Papers 480, 75–94. https://doi.org/10.1130/2011.2480(03)

Parlak, O., Dunkl, I., Karaoğlan, F., Kusky, T.M., Zhang, C., Wang, L., Koepke, J., Billor, Z., Hames, W.E., Şimşek, E., Şimşek, G., Şimşek, T., Öztürk, S.E., 2019. Rapid cooling history of a Neotethyan ophiolite: Evidence for contemporaneous subduction initiation and metamorphic sole

formation. GSA Bulletin 131, 2011–2038. https://doi.org/10.1130/B35040.1

Petroccia, A., Carosi, R., Montomoli, C., Iaccarino, S., Vitale Brovarone, A., 2022. Deformation and temperature variation along thrust-sense shear zones in the hinterland-foreland transition zone of collisional settings: A case study from the Barbagia Thrust (Sardinia, Italy). Journal of Structural Geology 161, 104640. https://doi.org/10.1016/j.jsg.2022.104640

Philpotts, A.R. and Ague, J.J. 2022. Principles of Igneous and Metamorphic Petrology, 3rd ed. DOI: 10.1017/9781108631419

Pomonis, P., Tsikouras, B., Hatzipanagiotou, K., 2002. Origin, evolution and radiometric dating of subophiolitic metamorphic rocks from the Koziakas ophiolite (W. Thessaly, Greece). Neues Jahrbuch Für Mineralogie, Abhandlungen 177, 255–276. https://doi.org/10.1127/0077-7757/2002/0177-0255

Ranalli, G., 1995. Rheology of the Earth, 2nd ed. Chapman and Hall. doi:10.1017/S0016756897226981

Rassios, A.E., Dilek, Y., 2009. Rotational deformation in the Jurassic Mesohellenic ophiolites, Greece, and its tectonic significance. Lithos 108, 207–223. https://doi.org/10.1016/j.lithos.2008.09.005

Rassios, A.H.E., Moores, E.M., 2006. Heterogeneous mantle complex, crustal processes, and obduction kinematics in a unified Pindos-Vourinos ophiolitic slab (northern Greece). Geological Society, London, Special Publications 260, 237. https://doi.org/10.1144/GSL.SP.2006.260.01.11

Reitan, P.H., 1968. Frictional heat during metamorphism: Quantitative evaluation of concentration of heat generation in time. Lithos 1, 151–163. https://doi.org/10.1016/S0024-4937(68)80005-2

Renshaw, C.E., Schulson, E.M., 2017. Strength-limiting mechanisms in high-confinement brittle-like failure: Adiabatic transformational faulting. Journal of Geophysical Research: Solid Earth 122, 2016JB013407. https://doi.org/10.1002/2016JB013407

Rioux, M., Garber, J., Bauer, A., Bowring, S., Searle, M., Kelemen, P., Hacker, B., 2016. Synchronous formation of the metamorphic sole and igneous crust of the Semail ophiolite: New constraints on the tectonic evolution during ophiolite formation from high-precision U-Pb zircon geochronology. Earth and Planetary Science Letters 451, 185–195. https://doi.org/10.1016/j.epsl.2016.06.051

Rybacki, E., Dresen, G., 2004. Deformation mechanism maps for feldspar rocks. Tectonophysics 382, 173–187. https://doi.org/10.1016/j.tecto.2004.01.006

Spray, J.G., 1984. Possible causes and consequences of upper mantle decoupling and ophiolite displacement. Geological Society, London, Special Publications 13, 255. https://doi.org/10.1144/GSL.SP.1984.013.01.21

Spray, J.G., Roddick, J.C., 1980. Petrology and 40Ar/39Ar geochronology of some hellenic sub-ophiolite metamorphic rocks. Contributions to Mineralogy and Petrology 72, 43–55. https://doi.org/10.1007/BF00375567

Stüwe, K., 2007. Geodynamics of the Lithosphere, 2nd ed. Springer-Verlag Berlin Heidelberg.

Stüwe, K., Ehlers, K., 1998. Distinguishing Cooling Histories using Thermometry. Interpretations of Cooling Curves with some Examples from the Glein-Koralm Region and the Central Swiss Alps. Mitteilungen Der Österreichischen Geologischen Gesellschaft 89, 201–212.

Stüwe, K. 1998. Heat sources of Cretaceous metamorphism in the Eastern Alps — a discussion. Tectonophysics, 287, 251–269, https://doi.org/10.1016/S0040-1951(98)80072-3.

Tsenn, M.C., Carter, N.L., 1987. Upper limits of power law creep of rocks. Tectonophysics 136, 1–26. https://doi.org/10.1016/0040-1951(87)90332-5

Vardoulakis, I., 2002. Steady shear and thermal run-away in clayey gouges. International Journal of Solids and Structures 39, 3831–3844. https://doi.org/10.1016/S0020-7683(02)00179-8

Wakabayashi, J., Dilek, Y., 2003. What constitutes 'emplacement' of an ophiolite?: Mechanisms and relationship to subduction initiation and formation of metamorphic soles. Geological Society, London, Special Publications 218, 427–447. https://doi.org/10.1144/GSL.SP.2003.218.01.22

Wakabayashi, J., Dilek, Y., 2000. Spatial and temporal relationships between ophiolites and their metamorphic soles: A test of models of forearc ophiolite genesis. In: Dilek, Y., Moores, E.M., Elthon, D., Nicolas, A. (Eds.), Ophiolites and Oceanic Crust: New Insights from Field Studies and the Ocean Drilling Program. Geological Society of America, 0. https://doi.org/10.1130/0-8137-2349-3.53

Whitechurch, H., Parrot, J., 1978. Ecailles métamorphiques infrapéridotiques dans le Pinde septentrional (Grèce): croûte océanique, métamorphisme et subduction. Comptes Rendus de l'Académie Des Sciences Paris 286, 1491–1494.

Whitechurch, H., Parrot, J.F., 1974. Les écailles métamorphiques infrapéridotitiques du Baër-Bassit (nord-ouest de la Syrie). Cah. ORSTOM, Sér. Géol. VI, 173–184.

Williams, H., Smyth, W.R., 1973. Metamorphic aureoles beneath ophiolite suites and alpine peridotites; tectonic implications with west Newfoundland examples. American Journal of Science 273, 594–621. https://doi.org/10.2475/ajs.273.7.594

Woodcock, N.H., Robertson, A.H.F., 1977. Origins of some ophiolite-related metamorphic rocks of the "Tethyan" belt. Geology 5, 373–376. https://doi.org/10.1130/0091-7613(1977)5<373:OOSOMR>2.0.CO;2

Young, J., 2015. Heat, work and subtle fluids: a commentary on Joule (1850) 'On the mechanical equivalent of heat.' Philosophical Transactions of the Royal Society A: Mathematical, Physical and Engineering Sciences 373, 20140348. https://doi.org/10.1098/rsta.2014.0348

Yuen, D.A., Fleitout, L., Schubert, G., Froidevaux, C., 1978. Shear deformation zones along major transform faults and subducting slabs. Geophysical Journal of the Royal Astronomical Society 54, 93–119. https://doi.org/10.1111/j.1365-246X.1978.tb06758.x

Received: 18.12.2023
Accepted: 9.2.2024
Editorial Handling: Kurt Stüwe